Dynamics of light harvesting in ZnO nanoparticles

2010 Nanotechnology 21 265703

(http://iopscience.iop.org/0957-4484/21/26/265703)

Nanotechnology **21** (2010) 265703 (5pp) doi:10.1088/0957-4484/21/26/265703

Dynamics of light harvesting in ZnO nanoparticles

Abhinandan Makhal[1], Soumik Sarkar[1], Tanujjal Bora[2], Sunandan Baruah[2], Joydeep Dutta[2], A K Raychaudhuri[1] and Samir Kumar Pal[1]

[1] Unit for Nano Science and Technology, S N Bose National Centre for Basic Sciences, Block JD, Sector III, Salt Lake, Kolkata 700 098, India
[2] Centre of Excellence in Nanotechnology, School of Engineering and Technology, Asian Institute of Technology, Klong Luang, Pathumthani 12120, Thailand

E-mail: joy@ait.asia, arup@bose.res.in and skpal@bose.res.in

Received 25 February 2010, in final form 13 May 2010
Published 4 June 2010
Online at stacks.iop.org/Nano/21/265703

Abstract
We have explored light harvesting of the complex of ZnO nanoparticles with the biological probe Oxazine 1 in the near-infrared region using picosecond-time-resolved fluorescence decay studies. We have used ZnO nanoparticles and Oxazine 1 as a model donor and acceptor, respectively, to explore the efficacy of the Förster resonance energy transfer (FRET) in the nanoparticle–dye system. It has been shown that FRET from the states localized near the surface and those in the bulk of the ZnO nanoparticles can be resolved by measuring the resonance efficiency for various wavelengths of the emission spectrum. It has been observed that the states located near the surface for the nanoparticles (contributing to visible emission at $\lambda \approx 550$ nm) can contribute to very high efficiency (>90%) FRET. The efficiency of light harvesting dynamics of the ZnO nanorods has also been explored in this study and they were found to have much less efficiency (∼40%) for energy transfer compared to the nanoparticles. The possibility of an electron transfer reaction has been ruled out from the picosecond-resolved fluorescence decay of the acceptor dye at the ZnO surface.

(Some figures in this article are in colour only in the electronic version)

1. Introduction

An efficient light harvesting step is critical for the success of various biologically important processes including photosynthesis, where rapid excitation energy transfer from the outer antenna to the reaction centre is required to compete with normal excited state quenching [1]. However, the precise molecular principles that enable such high efficiency have remained elusive because of the lack of both experimental and theoretical tools that can unambiguously reveal coupling and dynamics of the multi-chromophoric system [2]. In recent years harvesting of solar energy has attracted a lot of attention due to the realization of dye-sensitized solar cells (DSSCs) [3]. The decisive use of various sensitizers including quantum dots in the system is found to be one of the key considerations in the fabrication of efficient DSSCs [4] for the efficient transfer of solar energy from the sensitizers to the nanoparticulate film of a wide bandgap oxide semiconductor and eventually the charge separation determines the quality of the DSSCs. Extensive studies in order to quantify the efficacy of the energy transfer in various multi-chromophoric systems in proteins and DNA have been reported from our group [5, 6]. In a recent study, we have explored the ultrafast dynamics of the excitonic energy from a CdSe/ZnS quantum dot to a chemotherapeutic drug, merocyanine [7], by using Förster resonance energy transfer (FRET). It is also evident from the recent literature that FRET serves as a popular signal transduction mechanism to develop biosensing systems and bioassays for proteins, peptides, nucleic acids and small molecules [8–13]. Although the use of ZnO nanoparticles in DSSCs [14] and photolytic agents [15] are well documented in the literature, the reports on the light harvesting mechanism of nanoparticles are sparse. Here we report our studies on the ultrafast dynamics of energy transfer from zinc oxide nanoparticles (ZnO NP) to a well-known biological marker, Oxazine 1 (OX1) [16]. The cationic OX1 dye is supposed to bind at the surface of the n-type

ZnO NP. Picosecond-resolved FRET studies of the ZnO–OX1 system confirm that the surface states of the NPs contribute to the light harvesting process.

2. Materials and methods

Zinc acetate dihydrate ($(CH_3COO)_2Zn$, $2H_2O$) Merck, sodium hydroxide (NaOH) Merck, ethanol (C_2H_5OH) J T Baker, methanol (CH_3OH) Merck, isopropanol ($(CH_3)_2CHOH$) Lab Scan and Oxazine 1 (Exciton) are used as received without further purification. A ZnO nanoparticle colloidal solution in ethanol was synthesized following our earlier reports [15, 17, 18]. 4 mM zinc acetate solution and a 4 mM NaOH solution were prepared, both in ethanol under rigorous stirring at 50 °C. 20 ml of zinc acetate solution was complexed with 20 ml of pure ethanol and heat treated at 70 °C for half an hour. 20 ml of the NaOH solution was then added and the mixture solution was then hydrolyzed for 3 h at 60 °C. The ZnO–OX1 adduct was prepared by mixing the ZnO colloidal solution with a pre-calculated amount of OX1 and stirred for about 3 h in the dark prior to any measurements. A detailed structural study including monocrystalline properties of the nanoparticles is reported in our earlier publications [15, 18, 19]. Scanning electron microscopy (SEM) images were taken using a JEOL JSM-6301F operated at 20 kV. Transmission electron microscopy images were taken using a JEOL/JEM 2010 operated at 200 kV.

Steady state absorption and emission spectra were measured with a Shimadzu UV-2450 spectrophotometer and a Jobin Yvon Fluoromax-3 fluorimeter, respectively. All the photoluminescence transients were taken using the picosecond-resolved time-correlated single-photon counting (TCSPC) technique. We used a commercially available picosecond diode laser-pumped (LifeSpec-ps) time-resolved fluorescence spectrophotometer from Edinburgh Instruments, UK. The picosecond excitation pulse from the picoquant diode laser was used at 375 nm with an instrument response function (IRF) of 80 ps. A microchannel-plate photomultiplier tube (MCP-PMT, Hamamatsu was used to detect the photoluminescence from the sample after dispersion through a monochromator. For all transients the polarizer on the emission side was adjusted to be at 55° (magic angle) with respect to the polarization axis of the excitation beam. The observed fluorescence transients were fitted by using a nonlinear least-squares fitting procedure to a function ($X(t) = \int_0^t E(t')R(t-t')\,\mathrm{d}t'$) comprising of a convolution of the IRF ($E(t)$) with a sum of exponentials ($R(t) = A + \sum_{i=1}^{N} B_i \mathrm{e}^{-t/\tau_i}$) with pre-exponential factors (B_i), characteristic lifetimes (τ_i) and a background (A). Relative concentration in a multi-exponential decay is finally expressed as $c_n = \frac{B_n}{\sum_{i=1}^{N} B_i} \times 100$. The average lifetime (amplitude-weighted) of a multi-exponential decay [20] is expressed as $\tau_{\mathrm{av}} = \sum_{i=1}^{N} c_i \tau_i$.

In order to estimate fluorescence resonance energy transfer efficiency of the donor (ZnO) and hence to determine the distance of donor–acceptor pairs, we followed the methodology described in [19]. The Förster distance (R_0) is given by

$$R_0 = 0.211 \times [\kappa^2 n^{-4} Q_{\mathrm{D}} J]^{\frac{1}{6}} \text{ (in Å)} \tag{1}$$

where κ^2 is a factor describing the relative orientation in space of the transition dipoles of the donor and acceptor. For donor and acceptors that randomize by rotational diffusion prior to energy transfer, the magnitude of κ^2 is assumed to be 2/3. The refractive index (n) of the medium is assumed to be 1.4. Q_{D}, the integrated quantum yield of the donor in the absence of an acceptor, is measured to be 3.8×10^{-3}. J, the overlap integral, which expresses the degree of spectral overlap between the donor emission and the acceptor absorption, is given by

$$J = \frac{\int_0^\infty F_{\mathrm{D}}(\lambda)\varepsilon_{\mathrm{A}}(\lambda)\lambda^4\,\mathrm{d}\lambda}{\int_0^\infty F_{\mathrm{D}}(\lambda)\,\mathrm{d}\lambda} \tag{2}$$

where $F_{\mathrm{D}}(\lambda)$ is the fluorescence intensity of the donor in the wavelength range of λ to $\lambda + \mathrm{d}\lambda$ and is dimensionless; $\varepsilon_{\mathrm{A}}(\lambda)$ is the extinction coefficient (in $\mathrm{M}^{-1}\,\mathrm{cm}^{-1}$) of the acceptor at λ. If λ is in nm, then J is in units of $\mathrm{M}^{-1}\,\mathrm{cm}^{-1}\,\mathrm{nm}^4$. The estimated value of the overlap integral is 3.79×10^{15}.

Once the value of R_0 is known, the donor–acceptor distance (r_{DA}) can be easily calculated using the formula

$$r_{\mathrm{DA}}^6 = \frac{[R_0^6(1-E)]}{E}. \tag{3}$$

Here E is the efficiency of energy transfer. The transfer efficiency is measured using the relative fluorescence lifetime of the donor, in the absence (τ_{D}) and presence (τ_{DA}) of the acceptor:

$$E = 1 - \frac{\tau_{\mathrm{DA}}}{\tau_{\mathrm{D}}}. \tag{4}$$

We are also interested in obtaining the thickness of the surface layer emitting visible light by using a simple model [21]. In order to obtain the below-bandgap (550 nm, i.e. 2.25 eV) and near-band-edge (365 nm, i.e. 3.39 eV) emission of the ZnO nanoparticles, we have excited the sample with 320 nm (3.87 eV) light. The luminescence peak intensity ratio of the near-band-edge (NBE) to below-bandgap (BBG) emission for spherical particles of radius r and with a surface recombination layer of thickness t is given by [22]

$$\frac{I_{\mathrm{NBE}}}{I_{\mathrm{BBG}}} = C\left(\frac{r^3}{3rt(r-t)+t^3} - 1\right). \tag{5}$$

The constant C, along with other quantities, contains the oscillator strengths which in turn depend on the particle morphology. In order to calculate t from the above equation we have taken the magnitude of C as 3.89 for small spherical particles [22] with radius $r \approx 3$ nm. In our system $I_{\mathrm{NBE}}(365\text{ nm})/I_{\mathrm{BBG}}(550\text{ nm}) \approx 0.853$. Putting the values in equation (5) the thickness of the surface layer, t, was found to be 1.30 nm. It represents an effective distance from the surface (effective diffusion length), within which the excited carriers recombine at the surface.

3. Results and discussion

The absorption and emission spectra of ZnO (energy donor) and Oxazine 1 (energy acceptor) are shown in figure 1. It is clearly evident from the broad emission peak of the ZnO

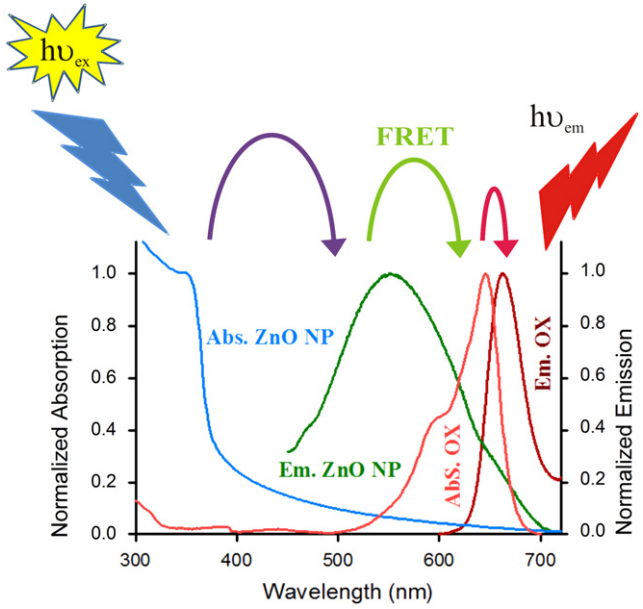

Figure 1. Normalized absorption (blue) and emission (green) spectra of ZnO NP with radius ∼3 nm. Cascade harvesting of blue photon to red photon in the ZnO NP–OX1 complex is shown. The normalized absorption and emission of OX1 are shown.

nanoparticles in ethanol at 550 nm that the photoluminescence is essentially dominated by the excitonic transition at the surface of the ZnO nanoparticles and defect-mediated origin of the green luminescence [22, 23]. van Dijken *et al* [24] proposed that the visible emission is due to the recombination of an electron from the conduction band with a deep electron trapping centre of V_O^{++}, which is considered as an oxygen vacancy centre. Alternatively, Vanheusden *et al* [25] suggested that the recombination of isolated V_O^{+} centres with photoexcited holes are responsible for the green emission. Because of the large surface-to-volume ratio of our ZnO nanoparticles, efficient and fast trapping of photogenerated holes at surface sites can be expected. However, the broad emission band can be decomposed into two components. The predominant emission energy is concentrated around the $\lambda = 550$ nm (2.25 eV) line while another emission band occurs at around $\lambda = 495$ nm (2.50 eV). It has been reported that the emission centre around 550 nm occurs from defect states near the surface layer (within a shell of t) while the shorter wavelength 495 nm emission occurs from defects near the bulk of the nanoparticles [21, 22, 26], which is located inside at a distance $>t$ from the surface. As the size of the nanoparticle is increased, the relative contribution of the 495 nm emission increases [22]. The absorption and emission spectra of the acceptor OX1 at the surface are also consistent with that reported in the literature [16]. The consistency of the spectral pattern of the acceptor OX1 with the other studies clearly rules out the possibility of any damage of the OX1 molecule at the ZnO surface. The spectral overlap of the ZnO emission spectrum with that of the OX1 absorption spectrum is shown in figure 2(a). The faster excited state lifetime of the ZnO–OX1 adduct with respect to that of the free ZnO NP is clearly noticeable from figure 2(b). The baseline uplift comes

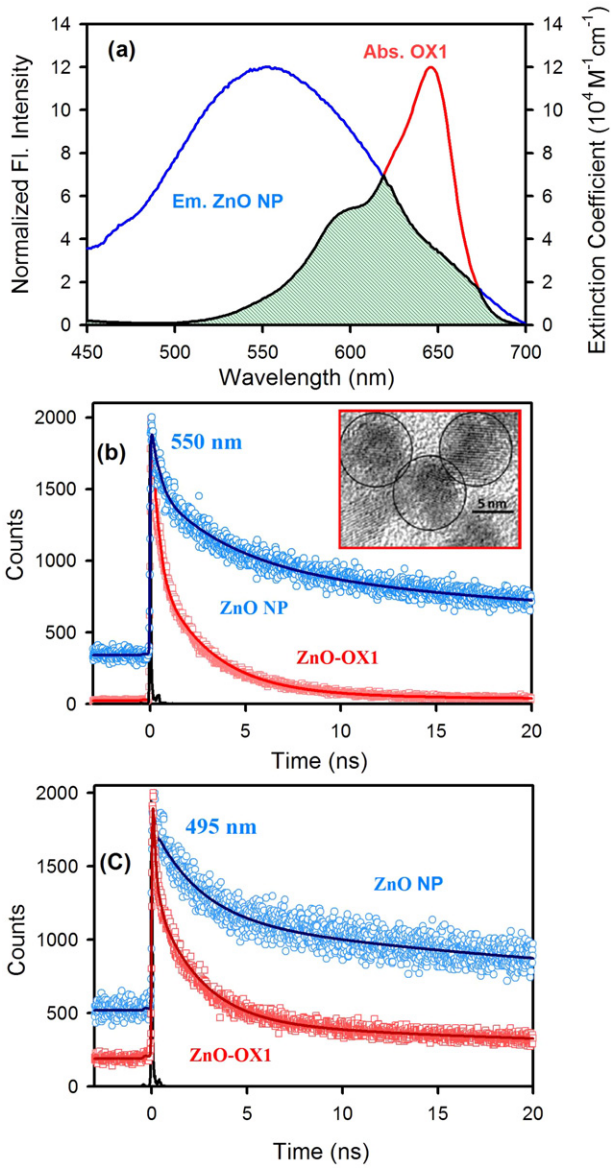

Figure 2. (a) Steady state absorption spectra of OX1 (red) and emission spectra of ZnO NP (blue) are shown. An overlapping zone between emission of ZnO NP and absorption of acceptor OX1 is indicated as a green shaded zone. The picosecond-resolved fluorescence transients of ZnO NP, in the absence (blue) and in the presence of acceptor OX1 (red) (excitation at 375 nm) collected at (b) 550 nm and (c) 495 nm, are shown. Inset of (b) shows the high resolution transmission electron microscope (HRTEM) image of ZnO nanoparticles.

from the long lifetime component which is not ending in our experimental time window.

The details of the spectroscopic parameters and the fitting parameters of the fluorescence decays are tabulated in table 1. From the average lifetime calculation for the ZnO–OX1 complex, we obtain the effective distance between the donor and the acceptor, $r_{DA} \approx 1.58$ nm, using equations (3) and (4). It is noted that r_{DA} is much smaller than the radius of the nanoparticle (∼3 nm; inset figure 2(b)) and is comparable to the thickness t of the surface layer of the nanoparticles, i.e. $r > r_{DA} \approx t$. In the case of organic acceptor molecules at the surface of a semiconductor (CdSe)

Table 1. Picosecond-resolved luminescence transients of various samples. The emission from ZnO nanoparticles (emission at 495 and 550 nm) was detected with 375 nm excitation. The emission of the acceptor OX1 in ethanol and at ZnO surface (emission at 665 nm) was detected with 633 nm laser excitation. Numbers in the parentheses indicate relative weightage.

Sample	τ_1 (ns)	τ_2 (ns)	τ_3 (ns)	τ_{av} (ns)
ZnO NP (550 nm)	47.583 ± 0.75 (40%)	3.787 ± 0.19 (23%)	0.281 ± 0.003 (37%)	20.32
ZnO NP–OX1 (550 nm)	19.044 ± 0.73 (1.4%)	2.797 ± 0.02 (33.3%)	0.259 ± 0.005 (65.3%)	1.37
ZnO NP (495 nm)	35.05 ± 0.87 (30%)	2.48 ± 0.15 (30%)	0.089 ± 0.009 (40%)	11.29
ZnO NP–OX1 (495 nm)	32.530 ± 0.39 (10%)	2.320 ± 0.02 (36%)	0.148 ± 0.006 (54%)	4.17
ZnO nanorod (495 nm)	10.372 ± 0.09 (6.3%)	2.440 ± 0.02 (28.2%)	0.159 ± 0.004 (65.5%)	1.45
ZnO rod-Ox1 (495 nm)	8.454 ± 0.06 (5.1%)	1.515 ± 0.01 (21.0%)	0.087 ± 0.003 (73.9%)	0.82
OX1 in EtOH (665 nm)	0.693 ± 0.001 (100%)	—	—	0.693
ZnO NP–OX1 (665 nm)	0.867 ± 0.002 (100%)	—	—	0.867

quantum dot donor, the overall donor–acceptor distance is reported to be nearly equal to (or larger than) the radius of the donor quantum dot [7]. The relatively shorter donor–acceptor distance in the case of the ZnO–OX1 system compared to other systems [7] can be rationalized from the fact that the origin of the photoluminescence peaking at 550 nm is essentially from the surface layer of an approximate thickness 1.3 nm of the ZnO nanoparticles.

In order to compare the FRET from other emission centres (scheme 1) of ZnO nanoparticles, we have also studied the energy transfer dynamics at $\lambda_{em} = 495$ nm. The relative dynamical quenching of the ZnO–OX1 system with respect to free ZnO at 495 nm is shown in figure 2(c). The relevant data are also given in table 1. From the average lifetime data and using equations (3) and (4) we obtain for the 495 nm emission $r_{DA} = 2.25$ nm, which is much larger than that observed at 550 nm. In this case $r \approx r_{DA} > t$, clearly indicating that the emission at 495 nm is from defect sites located within the bulk of the nanoparticles. The efficiency of the FRET (E) as obtained from equation (4) is highest for the 550 nm line (93%) and much smaller (63%) for the 495 nm line.

We have extended our studies on the attachment of the OX1 molecules at the surface of the ZnO nanorods. Nanorods are very important components for the state-of-the-art ZnO-based DSSC [27]. The morphology of a ZnO nanorod was characterized by SEM. A typical SEM image of a ZnO nanorod (figure 3(b) inset) shows 400 nm long and 40 nm wide nanorod growths. The nanorods are found to offer photoluminescence peaking at 495 nm. The spectral characteristic is consistent with the fact that the emission is dominated by the bulk state of the semiconductor [22, 28]. As shown in figure 3(b), the fluorescence quenching of the ZnO nanorod–OX1 adduct offers insignificantly small quenching with efficiency 44% compared to that of the free nanorods in the bulk ethanol. No attempt has been made to estimate donor–acceptor distance in the case of the nanorod–OX1 adduct because of the inadequate quantum yield of the ZnO nanorods.

Our experiments also explore the possibility of charge transfer from the ZnO surface. The acceptor molecule OX1 is

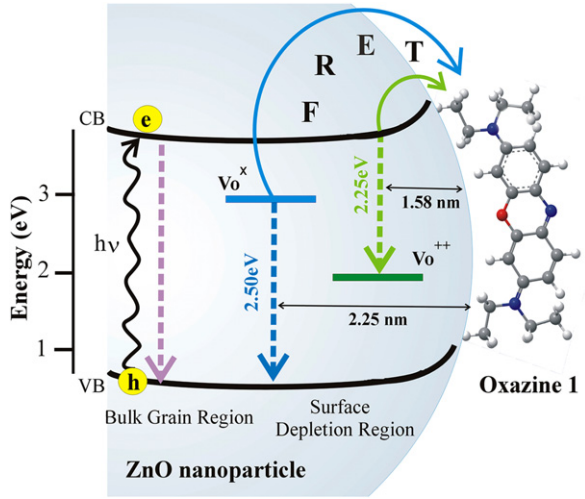

Scheme 1. Schematic diagram of ZnO NP–OX1 nanocomposite depicting the FRET dynamics from different oxygen vacancy centres (V_O^{++}, $V_O^{\times}$) of ZnO NPs to OX1 molecules. A singly charged oxygen vacancy centre (V_O^{+}), present in the surface depletion region, captures a hole to generate V_O^{++} centres, leading to an emission with a peak in the vicinity of 2.25 eV (550 nm). In the absence of a depletion region V_O^{+} becomes a neutral centre ($V_O^{\times}$) by capturing one electron from the conduction band which is responsible for an emission at 2.50 eV (495 nm). Typical FRET distances from different energy states of ZnO NPs to surface adsorbed OX1 are also shown. The bandgap excitation (3.87 eV, i.e. 320 nm) is shown by curved arrows.

well known to be a potential electron acceptor [16]. It has been demonstrated that the molecule offers an ultrafast fluorescence decay following an electron transfer reaction [29]. However, from figure 3(a) it is evident that the fluorescence decay of OX1 at the ZnO surface is slightly longer than that in the bulk ethanol. The observation clearly rules out the possibility of any kind of electron transfer reaction in the quenching process of the ZnO nanoparticles. On the other hand, slight lengthening of the excited state lifetime of the acceptor molecule OX1 confirms its adsorption at the ZnO surface [16], which makes the OX1 molecule more restricted.

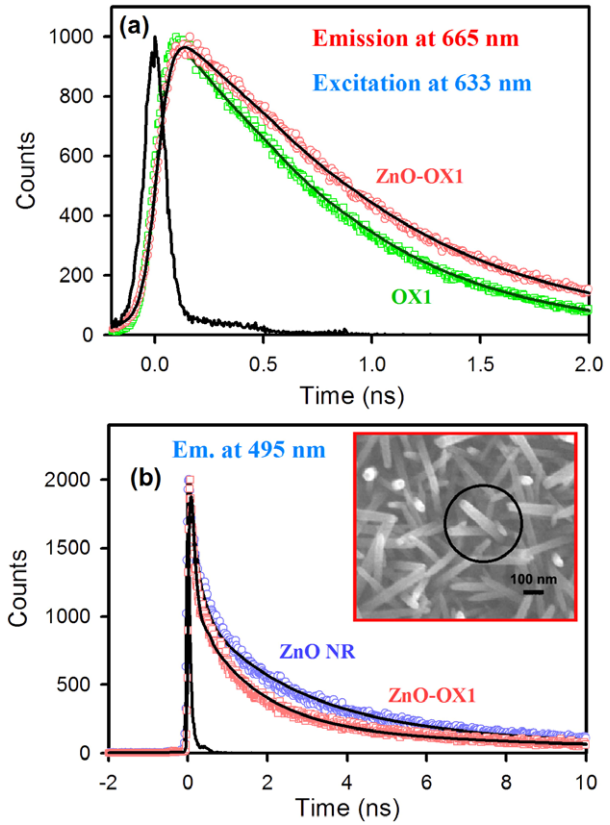

Figure 3. (a) The picosecond-resolved fluorescence transients of acceptor OX1 (green) and OX1 in the presence of ZnO NP (red), (excitation at 633 nm) collected at 665 nm. (b) Time-resolved quenching spectrum of ZnO nanorod in the presence (red) and the absence (blue) of OX1 (excitation at 375 nm) collected at 495 nm. Inset of the figure shows the scanning electron microscope (SEM) image of a ZnO nanorod.

4. Conclusion

In summary, we have explored the dynamics of light harvesting of ZnO nanoparticles in the near-infrared region. We have shown that, at the emission peak (550 nm) of the ZnO NP–Oxazine 1 adduct, efficient FRET (∼93%) occurs from surface state emission to the acceptor Oxazine 1 chromophore. The overall picture that evolved from our studies is summarized in scheme 1. Comparatively less efficient (63%) dynamics of the light harvesting of the ZnO nanoparticles from the emission peaking at 495 nm arises due to the defect sites located within the bulk of the nanoparticles. This can be separated from that of the emission obtained at 550 nm which originates from the below-bandgap emission at the surface of the nanoparticles. It is to be noted that the FRET distance (r_{DA}) is dependent on the emission wavelength of ZnO NPs whether it arises from surface or near-bulk states. Therefore, r_{DA} can be interpreted as a parameter that signifies the distance between the probe (OX1) and the different vacancy states of ZnO NPs. The possibility of the electron transfer reaction is ruled out from the picosecond-resolved fluorescence decay of the acceptor OX1 molecules at the ZnO surface. We have also shown that the efficiency of the ZnO nanoparticles as light harvesting material is much higher (efficiency 93%) than that of the nanorods. Our experimental observations may find relevance in the light harvesting devices using ZnO nanoparticles.

Acknowledgments

AM thanks CSIR and SS thanks UGC for fellowships. We thank DST for financial grants SR/SO/BB-15/2007 and Indo-Thailand Project DST/INT/THAI/P06/2008 and also for financial support for the Unit in Nanoscience. The authors (JD, SB, TB) would like to acknowledge partial financial support from the Centre of Excellence in Nanotechnology at the Asian Institute of Technology and the National Nanotechnology Center (NANOTEC) belonging to the National Science & Technology Development Agency (NSTDA), Thailand.

References

[1] Duysens L 1964 *Prog. Biophys. Mol. Biol.* **14** 101–4
[2] Cheng Y C and Fleming G R 2009 *Annu. Rev. Phys. Chem.* **60** 241–62
[3] Grätzel M 2004 *J. Photochem. Photobiol.* A **164** 3–14
[4] Kamat P V 2008 *J. Phys. Chem.* C **112** 18737–53
[5] Narayanan S S, Sinha S S, Verma P K and Pal S K 2008 *Chem. Phys. Lett.* **463** 160–5
[6] Banerjee D and Pal S K 2007 *J. Phys. Chem.* B **111** 5047–52
[7] Narayanan S S, Sinha S S and Pal S K 2008 *J. Phys. Chem.* C **112** 12716–20
[8] Scheller F W, Wollenberger U, Warsinke A and Lisdat F 2001 *Curr. Opin. Biotechnol.* **12** 35–40
[9] Iqbal S S, Mayo M W, Bruno J G, Bronk B V, Batt C A and Chambers J P 2000 *Biosens. Bioelectron.* **15** 549–78
[10] Morrison L E 1988 *Anal. Biochem.* **174** 101–20
[11] Whitcombe D, Theaker J, Guy S P, Brown T and Little S 1999 *Nat. Biotechnol.* **17** 804–7
[12] Cardullo R A, Agrawal S, Flores C, Zamecnik P C and Wolf D E 1988 *Proc. Natl Acad. Sci. USA* **85** 8785–9
[13] Ha T, Enderle T, Ogletree D F, Chemla D S, Selvin P R and Weiss S 1996 *Proc. Natl Acad. Sci. USA* **93** 6264–8
[14] Law M, Greene L E, Johnson J C, Saykally R and Yang P 2005 *Nat. Mater.* **4** 455–9
[15] Baruah S, Sinha S S, Ghosh B, Pal S K, Raychaudhuri A K and Dutta J 2009 *J. Appl. Phys.* **105** 074308
[16] Pal S K, Mandal D, Sukul D and Bhattacharyya K 1999 *Chem. Phys.* **249** 63–71
[17] Baruah S, Thanachayanont C and Dutta J 2008 *Sci. Technol. Adv. Mater.* **9** 025009
[18] Sugunan A, Warad H C, Boman M and Dutta J 2006 *J. Sol–Gel Sci. Technol.* **39** 49–56
[19] Baruah S and Dutta J 2009 *J. Cryst. Growth* **311** 2549–54
[20] Lakowicz J R 1999 *Principles of Fluorescence Spectroscopy* (New York: Kluwer Academic/Plenum)
[21] Shalish I, Temkin H and Narayanamurti V 2004 *Phys. Rev.* B **69** 245401
[22] Ghosh M and Raychaudhuri A K 2008 *Nanotechnology* **19** 445704
[23] Ye J D *et al* 2005 *Appl. Phys.* A **81** 759–62
[24] Dijken A V, Meulenkamp E A, Vanmaekelbergh D and Meijerink A 2000 *J. Lumin.* **87–89** 454–6
[25] Vanheusden K, Warren W L, Seager C H, Tallant D R and Voigt J A 1996 *J. Appl. Phys.* **79** 7983–90
[26] Kroger F A (ed) 1974 *The Chemistry of Imperfect Crystals* (Amsterdam: North-Holland)
[27] Jiang C Y, Sun X W, Lo G Q and Kwong D L 2007 *Appl. Phys. Lett.* **90** 263501
[28] Zheng Y, Chen C, Zhan Y, Lin X, Zheng Q, Wei K, Zhu J and Zhu Y 2007 *Inorg. Chem.* **46** 6675–82
[29] Shirota H, Pal H, Tominaga K and Yoshihara K 1998 *Chem. Phys.* **236** 355–64